



Cite this: *Dalton Trans.*, 2025, **54**, 11500

Received 12th May 2025,

Accepted 4th July 2025

DOI: 10.1039/d5dt01116g

rsc.li/dalton

Exploring the synthesis of a rare-earth cluster-based metal–organic framework using alternative yttrium(III) precursors†

Hudson A. Bicalho,^{a,b} Isabella Lopez-Delgado,^{a,c} Clara V. Diniz,^{a,b} Zoey Davis^{a,b} and Ashlee J. Howarth^{✉a,b}

The synthesis of rare-earth cluster-based MOFs is often performed using metal nitrate salts as precursors. In this work, we demonstrate that six other Y(III) precursors can be used as alternatives in the synthesis of Y-CU-45 (CU = Concordia University), yielding reproducible results and high-quality materials.

Metal–organic frameworks (MOFs) have emerged as an important class of materials, often displaying high crystallinity and surface area, permanent porosity, and tunable structures.¹ MOFs are constructed from inorganic metal nodes (ions, chains, or clusters) and multitopic organic linkers, which assemble into a framework material. The diversity of both inorganic and organic nodes that can be used to construct MOFs enables a seemingly limitless number of structural possibilities.²

In 2014, Furukawa *et al.*³ demonstrated, for the first time, that the linker 1,3,5-benzenetricarboxylic acid (H₃BTC) could be used to synthesize a Zr-based MOF with hexanuclear cluster nodes. This MOF received the name MOF-808 and, nowadays, it is one of the most studied MOFs in the literature.⁴ A part of its success can be attributed to the high thermal and chemical stability of MOF-808, a common attribute among many Zr(IV) cluster-based MOFs.⁵ MOF-808 also features a high surface area (>1600 m² g^{−1}) and porosity (pores of 8 and 18 Å), in addition to six open metal sites per cluster.³ Frequently, these open metal sites are coordinated to formate or acetate capping ligands, which can be removed by solvent or acid washing procedures to generate terminal and labile –OH and –OH₂ ligands in their place.⁶ Upon replacement of the capping ligands with terminal labile ligands, the open metal sites can be taken advantage of for multiple applications, often related to catalysis,⁷ adsorption,⁸ drug delivery,⁹ or gas separation.¹⁰

More recently, MOF-808 analogues consisting of tetravalent metals have been obtained, including Hf,¹¹ Ce,¹² and Th-MOF-808.¹³ Nevertheless, it was not until eight years after its original discovery that our group demonstrated an analogous structure to MOF-808 containing trivalent metals.¹⁴ In this previous work, we demonstrated that the rare-earth ion, Y(III), could be used to obtain a MOF that displays the same structure as MOF-808, featuring hexanuclear Y(III) clusters and the overall *spn* topology. This MOF, which can also be synthesized with lanthanoids ranging from Eu(III)–Lu(III),¹⁵ received the name RE-CU-45 (Fig. 1). Different from MOF-808, however, RE-CU-45 possesses bulky capping ligands coordinated to its open metal sites, such as 2,6-difluorobenzoate and trifluoroacetate, which ultimately partially block the pores of RE-CU-45, decreasing its surface area (~1200 m² g^{−1}) compared to MOF-808 (>1600 m² g^{−1}). We have demonstrated that these capping ligands can be partially removed through an acid washing procedure, without impacting the stability of the framework, leading to an increase in the surface area of Y-CU-45 from 1200 to 1600 m² g^{−1}.¹⁴

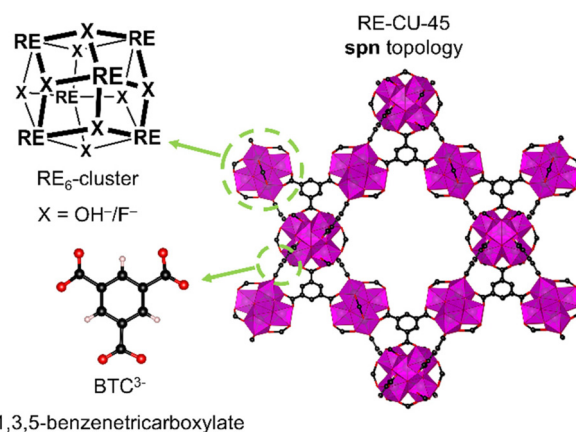


Fig. 1 Structure of RE-CU-45 consisting of hexanuclear RE(III) clusters and BTC^{3−} linkers.

^aDepartment of Chemistry and Biochemistry, Concordia University, 7141 Sherbrooke St W., Montréal, QC, Canada. E-mail: ashlee.howarth@concordia.ca

^bCentre for NanoScience Research, Concordia University, Montréal, QC, Canada

^cDepartamento de Química, Universidad del Valle, AA 25360 Cali, Colombia

† Electronic supplementary information (ESI) available. See DOI: <https://doi.org/10.1039/d5dt01116g>

In the RE-MOF literature, including our work with RE-CU-45, RE(III) nitrates are the most common precursors used for the synthesis of RE cluster-based MOFs.^{16,17} Alternatively, a few studies have employed RE(III) chlorides as precursors.¹⁸ In general, both RE(III) nitrate and chloride precursors present some challenges due to their highly hygroscopic nature, which can lead to the uncontrolled addition of water during MOF synthesis, limiting experimental control, and consequently leading to problems related to synthetic reproducibility. Moreover, there are increasing concerns associated with safety when metal nitrate precursors are used, related to their oxidative characteristics in the presence of flammable substances, such as *N,N*-dimethylformamide (DMF), as well as their toxicity.¹⁹ Metal nitrate precursors can also react with amines, such as dimethylamine that is produced through the decomposition of DMF, to form nitrosamines, which are toxic and carcinogenic species.²⁰ A viable alternative would be to use RE(III) precursors that are less hygroscopic, and low cost, with fewer environmental and physical hazards. Recently, our group has shown that RE-UiO-66 can be synthesized using RE(III) acetate precursors in place of RE(III) nitrates, which leads to materials with the same characteristics and quality as the ones obtained when RE(III) nitrate precursors are used.²¹

With that in mind, we have selected a list of ten different Y(III) precursors: Y(III) nitrate, chloride, sulfate, phosphate, formate, acetate, trifluoroacetate, oxalate, hydroxide, and oxide.²² To the best of our knowledge, only RE(III) nitrate,^{16,17} chloride,^{18,23} and acetate²¹ have been reported as precursors for the synthesis of RE cluster-based MOFs. As such, seven RE(III) precursors are being explored herein for the first time, for the synthesis of a rare-earth cluster-based MOF.

While Y(III) nitrate, chloride, acetate, sulfate, trifluoroacetate, and oxide are commercially available, the other Y(III) precursors are less common and not available from many chemical suppliers. In this way, we have synthesized the Y(III) precursors with hydroxide, formate, oxalate, and phosphate (Fig. S1–S5†). All reaction conditions for those syntheses can be found in the ESI.† To test whether these Y(III) precursors could be used to synthesize Y-CU-45, all precursors were added with the same molar ratio as that used in the original Y-CU-45 synthesis that employed Y(III) nitrate.¹⁴ In short, 0.31 mmol of the Y(III) precursor is mixed with 1.5 mmol of 2,6-difluorobenzoic acid (2,6-dFBA) and solubilized in 1.5 mL of DMF and 0.30 mL (3.9 mmol) of trifluoroacetic acid (TFA). To this solution, 0.065 mmol of H₃BTC is solubilized, and the solution is heated at 130 °C for 5 days. Finally, the obtained microcrystalline powders are washed multiple times with DMF and acetone, giving rise to Y-CU-45.¹⁴

While the reactions using Y(III) nitrate, chloride, formate, acetate, trifluoroacetate, hydroxide, and oxide yielded Y-CU-45 (Fig. 2), this was not the case for reactions using Y(III) sulfate, phosphate, or oxalate precursors (Fig. S6–S9†). When Y(III) sulfate was used, the precursor did not solubilize within 5 days of reaction, preventing the formation of any MOF products. However, the Y(III) sulfate was converted from Y₂(SO₄)₃·8H₂O to

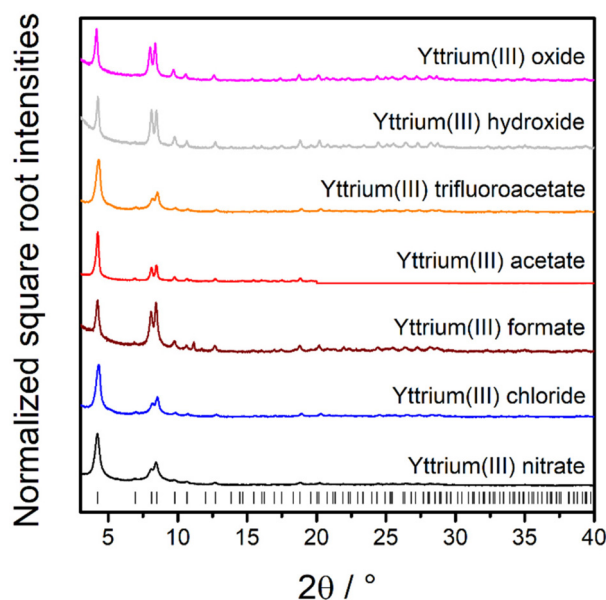


Fig. 2 PXRD patterns of Y-CU-45 obtained using different Y(III) precursors.

an unknown phase with both sulfate and BTC^{3−} present, but with no porosity (Fig. S6 and S7†). Similarly, the Y(III) phosphate precursor did not fully solubilize in the reaction media, and the final product indicates that the initial Y(PO₄)·2H₂O was still present at the end of the reaction (Fig. S8†). The presence of PO₄^{3−} ions is known to lead to the collapse of certain MOFs,²⁴ due to the high affinity of high valent metals for phosphate-based ligands. In the case of the synthesis of Y-CU-45, PO₄^{3−} may have prevented or slowed MOF formation due to competitive binding with Y(III), hindering the formation of hexanuclear Y-hydroxo or -fluoro clusters, and preventing the formation of Y-CU-45. While the Y(III) oxalate precursor solubilized in the first days of reaction, the higher content of oxalate ions, in comparison to BTC^{3−} (0.465 mmol versus 0.065 mmol, respectively), appeared to favour the formation of an oxalate-based MOF (Fig. S9†), that has been recently reported in the literature.²⁵ Heating this reaction for longer periods of time (7 days) led to a mixture of the Y(III)-oxalate MOF and Y-MOF-76,²⁶ a chain-based MOF containing BTC^{3−} linkers (Fig. S9†).

The remaining seven Y(III) precursors, however, enabled the formation of Y-CU-45, as can be seen in the powder X-ray diffraction (PXRD) patterns displayed in Fig. 2. The typical diffractogram for MOF-808/RE-CU-45 features the most intense reflection at 4.1° 2θ, corresponding to the (111) plane, followed by two intense reflections at 8.0 and 8.4° 2θ, which are assigned to the (311) and (222) planes, respectively.^{3,14} Slight changes in the intensity of these latter peaks can be attributed to the presence of residual solvent in the pores of the MOF (Fig. S10†). While Y(III) nitrate, chloride, acetate, and trifluoroacetate readily dissolved in the mixture containing DMF and TFA, Y(III) formate, hydroxide, and oxide only dissolved after a few days



of heating at 130 °C. In an initial attempt, it appeared that the synthesis of Y-CU-45 using Y(III) oxide was a success, as no diffraction peaks from the precursor were observed in the diffractogram (Fig. S11a†). However, additional characterization demonstrated that there was still some amorphous oxide leftover after the reaction was complete, with the resulting Y-CU-45 sample showing a BET surface area of only 480 m² g⁻¹ (Fig. S11b†), a substantial difference from what is expected, >1000 m² g⁻¹. Scanning electron microscopy (SEM) images also demonstrated the presence of bright white spheres, likely from leftover Y₂O₃ after the synthesis (Fig. S11c†). This was confirmed by thermogravimetric analysis (TGA), where a larger residual mass, compared to that expected for Y-CU-45, was observed (Fig. S11d†).

After several attempts at optimizing the reaction conditions for Y-CU-45 from the Y(III) oxide precursor, it was found that decreasing the amount of metal by 15% and increasing the amount of linker by 28%, giving a metal:linker ratio of 3:1 (down from a ratio of 4.85:1 in the typical procedure, and equivalent to the final ratio of metal:linker in Y-CU-45), leads to phase pure Y-CU-45. By doing that, the higher ratio of acids (linker and modulator) to metal seems to promote the dissolution of Y₂O₃ at high temperature, while also minimizing the use of excess metal in the synthesis. In this way, leftover Y₂O₃ was not observed by PXRD or SEM (Fig. S12a and S12b†). At the same time, Y-CU-45 obtained with the Y(III) oxide precursor showed a BET surface area of 1020 m² g⁻¹ (Fig. S12c†) and no considerable difference in thermal stability or residual mass by TGA (Fig. S12d†).

While the synthesis of Y-CU-45 using Y(III) oxide as a precursor required optimization to avoid the presence of leftover precursor after the synthesis, the other six Y(III) precursors could be used following the typical reaction conditions. These materials displayed BET surface areas of 1285, 1250, 1190, 1320, 1320, and 1300 m² g⁻¹, for Y(III) nitrate, chloride, formate, acetate, trifluoroacetate, and hydroxide, respectively (Fig. S13†). The precursors that led to the Y-CU-45 samples with the lowest surface areas, Y(III) formate (1190 m² g⁻¹) and Y(III) oxide (1020 m² g⁻¹), are also the ones that display the fewest number of capping ligands and μ_3 -F ligands in the Y₆-cluster (*vide infra*). This is consistent with our previous results showing that removing too many capping ligands from Y-CU-45 renders the MOF less stable to activation.¹⁴ All Y-CU-45 samples showed similar thermal stabilities, as observed by TGA (Fig. S14†), demonstrating decomposition of the linker starting at 530 °C. However, as previously described,¹⁴ Y-CU-45 begins losing crystallinity around 250 °C, due to the decomposition of the capping ligands on the cluster.¹⁴

As expected, all Y-CU-45 samples obtained using the different Y(III) precursors displayed an octahedral morphology. However, it can be noticed by SEM that the crystallites obtained when the Y(III) nitrate, chloride, acetate, and trifluoroacetate precursors were used are larger, while the Y-CU-45 crystallites from Y(III) formate, hydroxide, and oxide are smaller (Fig. 3 and Fig. S15†). Not coincidentally, these last three precursors are the ones that did not readily dissolve in

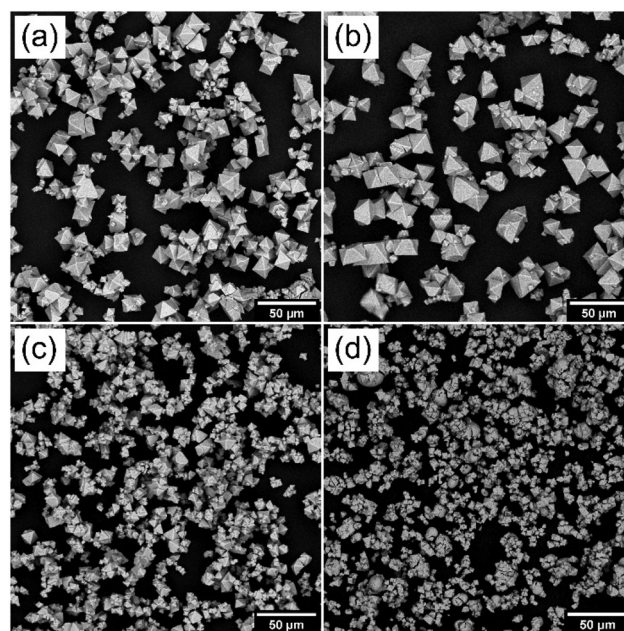


Fig. 3 SEM images of Y-CU-45 obtained from Y(III) (a) acetate, (b) trifluoroacetate, (c) formate, and (d) oxide precursors.

the reaction media, which may hamper both the nucleation and growth of the Y-CU-45 crystals due to the lack of Y(III) in solution. To gain a better understanding of the chemical environment of the Y₆-clusters, ¹H- and ¹⁹F-NMR spectroscopy was performed on digested samples of the MOFs. As can be seen in Tables S1 and S2† and Fig. S16–S22,† all Y₆-clusters are capped by the modulators used in the synthesis, 2,6-difluorobenzoate and trifluoroacetate, in addition to formate, which is formed due to the decomposition of DMF. It is interesting to note that Y₆-clusters in the Y-CU-45 samples made from more soluble Y(III) precursors show similar chemical composition, including the content of μ_3 -F bridges²⁷ in the cluster. In these MOFs, ratios of 2,6-dFBA:TFA:formate: μ_3 -F of 2.95:0.78:0.31:7.99, 2.92:1.23:0.06:7.26, 2.81:1.38:0.07:7.21, and 2.98:1.54:0.03:7.53 were obtained, when precursors of Y(III) nitrate, chloride, acetate, and trifluoroacetate were used, respectively. These results are in agreement with recent findings, where the content of μ_3 -F bridges in the cluster of RE-CU-45 are higher than 7 for Y(III) and the late lanthanoids.¹⁵ At the same time, when precursors of Y(III) formate, hydroxide, and oxide are used, ratios of 1.87:1.14:3.91, 3.25:0.99:6.39, and 1.75:0.45:3.63 were obtained, respectively, for 2,6-dFBA:TFA: μ_3 -F. These results not only indicate that the Y₆-clusters have fewer μ_3 -F bridges, but also that fewer capping ligands are coordinated to the clusters, especially when Y(III) formate and oxide precursors are used. These latter precursors also take more time to solubilize, in comparison to Y(III) hydroxide, which may lead to a slower rate of C–F bond activation and, consequently, Y(III)–F bond formation in the hexanuclear clusters.²⁸ Furthermore, when Y(III) acetate and trifluoroacetate precursors were used, these ligands were also



incorporated in the Y_6 -clusters, with a ratio of 0.12, and 1.54, respectively, to 2 BTC^{3-} linkers.

Given that metal-linker (MOF) or metal-ligand (precursor) bond strength can be correlated to the pK_a of the free linker/ligand,^{29–31} it is perhaps not surprising that Y-CU-45 could not be formed from Y(III) sulfate, phosphate, or oxalate precursors. As the pK_{a2} or pK_{a3} of sulphuric acid, phosphoric acid, and oxalic acid in DMF are >15 (Table S3†), their conjugate bases are expected to form stronger Y(III)-ligand bonds than those of Y(III) with the BTC^{3-} linker ($pK_{a1} = \sim 10.5$), the modulators (TFA $pK_a = 6.1$; 2,6-dFBA $pK_a = 9.91$), or the μ_3 -F ligands ($pK_a = \sim 15$). On the other hand, using this same logic it may not be clear why Y-CU-45 can be obtained from Y(III) oxide and hydroxide precursors. However, it is likely that these syntheses involve a Y(III) trifluoroacetate intermediate that is generated *in situ*, through the dissolution of the basic Y(III) oxide/hydroxide precursor in TFA, which is analogous to the standard conditions used to produce RE(III) trifluoroacetate precursors, as reported extensively in the literature.^{32,33}

In conclusion, we report the use of additional Y(III) precursors for the synthesis of Y-CU-45. While Y(III) nitrate was used for the original synthesis of Y-CU-45, we demonstrated that six other precursors could be successfully applied, leading to the synthesis of the targeted RE cluster-based MOF. Among these precursors, it should be highlighted that Y(III) oxide, an inexpensive and non-hygroscopic Y(III) source, can be used as a promising alternative for the synthesis of a RE cluster-based MOF. Additionally, depending on the chosen Y(III) precursor, slightly different properties can be obtained for the final material, including different crystallite sizes or different capping and bridging ligands on the Y_6 -clusters, which may be relevant for future applications of Y-CU-45 and other rare-earth cluster-based MOFs.

Author contributions

Hudson A. Bicalho – conceptualization, methodology, investigation, validation, visualization, project administration, writing – original draft; Isabella Lopez-Delgado – investigation, validation, visualization, writing – original draft; Clara V. Diniz – investigation, validation; Zoey Davis – investigation, validation; Ashlee J. Howarth – conceptualization, funding acquisition, project administration, resources, supervision, writing – review & editing.

Conflicts of interest

There are no conflicts to declare.

Data availability

Data for this article, including PXRD, BET, TGA, and NMR spectroscopy are available at Borealis: The Canadian Dataverse Repository at <https://doi.org/10.5683/SP3/RVNSBX>.

Acknowledgements

HAB and CVD thanks Concordia University and the Fonds de Recherche du Québec – Nature et technologies for providing doctoral scholarships. ILD acknowledges Mitacs for providing an exchange scholarship. We acknowledge the support of the Natural Sciences and Engineering Research Council of Canada (NSERC), [funding reference number: RGPIN-2024-04293]. Cette recherche a été financée par le Conseil de recherches en sciences naturelles et en génie du Canada (CRSNG), [numéro de référence: RGPIN-2024-04293]. We acknowledge the support of the Canada Foundation for Innovation (CFI) and the Ministère de l'Enseignement supérieur (MES) [application number: 43646]. All MOF figures were made using VESTA 3.

References

- 1 R. Freund, O. Zaremba, G. Arnauts, R. Ameloot, G. Skorupskii, M. Dincă, A. Bavykina, J. Gascon, A. Ejsmont, J. Goscińska, M. Kalmutzki, U. Lächelt, E. Ploetz, C. S. Diercks and S. Wuttke, *Angew. Chem., Int. Ed.*, 2021, **60**, 23975–24001.
- 2 H. Furukawa, K. E. Cordova, M. O'Keeffe and O. M. Yaghi, *Science*, 2013, **341**, 1230444.
- 3 H. Furukawa, F. Gándara, Y.-B. Zhang, J. Jiang, W. L. Queen, M. R. Hudson and O. M. Yaghi, *J. Am. Chem. Soc.*, 2014, **136**, 4369–4381.
- 4 G. Lee, I. Ahmed, M. A. Hossain, H. J. Lee and S. H. Jhung, *Coord. Chem. Rev.*, 2025, **524**, 216325.
- 5 M. Taddei, *Coord. Chem. Rev.*, 2017, **343**, 1–24.
- 6 E. Aunan, C. W. Affolter, U. Olsbye and K. P. Lillerud, *Chem. Mater.*, 2021, **33**, 1471–1476.
- 7 S.-Y. Moon, Y. Liu, J. T. Hupp and O. K. Farha, *Angew. Chem., Int. Ed.*, 2015, **54**, 6795–6799.
- 8 C. Copeman, H. A. Bicalho, M. W. Terban, D. Troya, M. Etter, P. L. Frattini, D. M. Wells and A. J. Howarth, *Chem. Commun.*, 2023, **59**, 3071–3074.
- 9 F. Demir Duman, A. Monaco, R. Foulkes, C. R. Becer and R. S. Forgan, *ACS Appl. Nano Mater.*, 2022, **5**, 13862–13873.
- 10 T. M. Rayder, F. Formalik, S. M. Vornholt, H. Frank, S. Lee, M. Alzayer, Z. Chen, D. Sengupta, T. Islamoglu, F. Paesani, K. W. Chapman, R. Q. Snurr and O. K. Farha, *J. Am. Chem. Soc.*, 2023, **145**, 11195–11205.
- 11 Y. Liu, R. C. Klet, J. T. Hupp and O. Farha, *Chem. Commun.*, 2016, **52**, 7806–7809.
- 12 M. Lammert, C. Glißmann, H. Reinsch and N. Stock, *Cryst. Growth Des.*, 2017, **17**, 1125–1131.
- 13 T. Islamoglu, D. Ray, P. Li, M. B. Majewski, I. Akpınar, X. Zhang, C. J. Cramer, L. Gagliardi and O. K. Farha, *Inorg. Chem.*, 2018, **57**, 13246–13251.
- 14 H. A. Bicalho, F. Saraci, J. d. J. Velazquez-Garcia, H. M. Titi and A. J. Howarth, *Chem. Commun.*, 2022, **58**, 10925–10928.
- 15 H. A. Bicalho, C. Copeman, H. P. Barbosa, P. R. Donnarumma, Z. Davis, V. Quezada-Novoa,



- J. d. J. Velazquez-Garcia, N. Liu, E. Hemmer and A. J. Howarth, *Chem. – Eur. J.*, 2024, **30**, e202402363.
- 16 H. A. Bicalho, L. A. Trifoi, V. Quezada-Novoa and A. J. Howarth, *ACS Appl. Electron. Mater.*, 2024, **6**, 7055–7064.
- 17 Y. Wang, L. Feng, W. Fan, K.-Y. Wang, X. Wang, X. Wang, K. Zhang, X. Zhang, F. Dai, D. Sun and H.-C. Zhou, *J. Am. Chem. Soc.*, 2019, **141**, 6967–6975.
- 18 S. E. Henkelis, D. J. Vogel, P. C. Metz, N. R. Valdez, M. A. Rodriguez, D. X. Rademacher, S. Purdy, S. J. Percival, J. M. Rimsza, K. Page and T. M. Nenoff, *ACS Appl. Mater. Interfaces*, 2021, **13**, 56337–56347.
- 19 H. Reinsch, *Eur. J. Inorg. Chem.*, 2016, **2016**, 4290–4299.
- 20 J. C. Donovan, K. R. Wright and A. J. Matzger, *Angew. Chem., Int. Ed.*, 2025, **64**, e202500531.
- 21 M. Richezzi, P. R. Donnarumma, C. Copeman and A. J. Howarth, *Chem. Commun.*, 2024, **60**, 5173–5176.
- 22 F. Ortu, *Chem. Rev.*, 2022, **122**, 6040–6116.
- 23 C. Liu, S. V. Eliseeva, T.-Y. Luo, P. F. Muldoon, S. Petoud and N. L. Rosi, *Chem. Sci.*, 2018, **9**, 8099–8102.
- 24 X. Chen, Y. Zhuang, N. Rampal, R. Hewitt, G. Divitini, C. A. O’Keefe, X. Liu, D. J. Whitaker, J. W. Wills, R. Jugdaohsingh, J. J. Powell, H. Yu, C. P. Grey, O. A. Scherman and D. Fairen-Jimenez, *J. Am. Chem. Soc.*, 2021, **143**, 13557–13572.
- 25 R. H. Alzard, L. A. Siddig, N. i. Saleh, H. L. Nguyen, Q. A. T. Nguyen, T. H. Ho, V. Q. Bui, K. Sethupathi, P. K. Sreejith and A. Alzamy, *Sci. Rep.*, 2022, **12**, 18812.
- 26 J. Luo, H. Xu, Y. Liu, Y. Zhao, L. L. Daemen, C. Brown, T. V. Timofeeva, S. Ma and H.-C. Zhou, *J. Am. Chem. Soc.*, 2008, **130**, 9626–9627.
- 27 J. P. Vizuet, M. L. Mortensen, A. L. Lewis, M. A. Wunch, H. R. Firouzi, G. T. McCandless and K. J. Balkus Jr., *J. Am. Chem. Soc.*, 2021, **143**, 17995–18000.
- 28 M. Abbas, S. Sheybani, M. L. Mortensen and K. J. Balkus, *Dalton Trans.*, 2024, **53**, 3445–3453.
- 29 V. Colombo, S. Galli, H. J. Choi, G. D. Han, A. Maspero, G. Palmisano, N. Masciocchi and J. R. Long, *Chem. Sci.*, 2011, **2**, 1311–1319.
- 30 H. J. Choi, M. Dincă, A. Dailly and J. R. Long, *Energy Environ. Sci.*, 2010, **3**, 117–123.
- 31 P. Lu, Y. Wu, H. Kang, H. Wei, H. Liu and M. Fang, *J. Mater. Chem. A*, 2014, **2**, 16250–16267.
- 32 J. E. Roberts, *J. Am. Chem. Soc.*, 1961, **83**, 1087–1088.
- 33 H.-X. Mai, Y.-W. Zhang, R. Si, Z.-G. Yan, L.-d. Sun, L.-P. You and C.-H. Yan, *J. Am. Chem. Soc.*, 2006, **128**, 6426–6436.

